Transactions, SMiRT-23
Manchester, United Kingdom - August 10-14, 2015
Division II, Paper ID 192
Fracture Mechanics and Structural Integrity

EC FP7 Structural Performance of MULTI-METAL AREVA GmbH Fracture toughness testing and interpretation on MU1 Part 2: interpretation

Elisabeth Keim[1], Sébastien Blasset[2], Stefan Heußner[3]

[1] Fracture Mechanics AREVA Fellow, AREVA GmbH, Technical Center Germany
[2] Analytical Fracture Mechanics, AREVA GmbH, Technical Center Germany
[3] Numerical Fracture Mechanics, AREVA GmbH, Technical Center Germany

ABSTRACT

The purpose of this paper is to present the interpretation of fracture toughness testing of standard specimens taken from the dissimilar metal welds mock-ups investigated at AREVA GmbH Technical Center labs in the frame of the MULTIMETAL project. Tests on standard fracture mechanics specimens have been performed, the specimens were taken from welded plate mock-up MU1 (narrow gap DMW with Ni-52). Several crack locations have been considered according to the experience from field (WP2). The interpretation of testing results by means of numerical investigation is summarized.

INTRODUCTION

Dissimilar metal welds (DMWs), such as joint welds between ferritic steels with either austenitic stainless steels or Nickel-base alloys, are commonly found in piping systems of nuclear power plants (NPPs) as well as in other industrial plants. Depending upon the specific application, these welds are usually produced using either austenitic stainless steel filler materials (electrodes) or nickel-base filler materials, manual or automatic welding process, and V grooved or Narrow gaps. Due to the large number of manufacturers and applied optimization methods, existing DMW configurations are numerous. In recent years some concerns have been raised about the reliability of DMWs, especially when the plant in focus is in operation beyond its initial design life. Integrity assessment of flaws in welds requires substantial material data like fracture toughness values, which are evaluated according to standards that are not necessarily foreseen for the weld configuration in focus. Thus, there is a need to develop a standard for toughness measurements in multi-metallic specimens.

RESULTS

CT12.5 specimens are manufactured from mock-up material specifically produced for this purpose and tested at room temperature in order to determine the tearing resistance of the material combination. Besides mechanical testing, additional examination techniques such as electron micrography and 3D macroscopy are applied to investigate the material behavior. This experimental analysis is presented in a parent paper at the SMIRT conference. A numerical analysis of one of the tested CT specimens is performed to verify the applicability of the J-integral method (as given in ASTM 1820-11) to inhomogeneous specimens.

Numerical analysis of CT12.5 specimen 2

CT12.5 specimens are manufactured from mock-up material specifically produced for this purpose and tested. A Finite Element (FE) analysis of CT12.5 specimen 2 is performed in order to verify the applicability of the procedure usually applied in the FE-code Abaqus for evaluating the J-integral in cracked structures consisting of homogenous materials to multi metallic specimens. Specimen 2 is modelled as a 3D model regarding the specific dimensions of this specimen, especially the pre-crack length. The general dimensions of the CT12.5 specimen are W = 25 mm, a_0 = 15,16 mm (a_0/W = 0.6064), and B_N = 10.022 mm. The specimen is fully modelled; geometrical symmetries are not exploited in this analysis. The mesh of the model is carried out with increasing element density in vicinity of the crack front which is modelled straight. The mesh of the model is performed with 20 node hexahedron elements with quadratic shape functions and reduced integration (C3D20R). The elements adjoining to the crack front are degenerated to wedge shape in order to facilitate a suitable mesh for reproducing the stress singularity and for the evaluation of the J-integral as the parameter of crack tip loading which is calculated via 25 paths along the crack front. The J-integral is peaking in the centre of the specimen due the ensuing stress state. For the evaluation of the analysis this maximum value is used.

The material assignments to the elements are made in accordance with the specimen extraction drawings. The settings for the numerical calculations within the MULTIMETAL projects are agreed among the partners and are adopted as well for this analysis. The analysis is performed with elastic-plastic material behaviour with the assumption of isotropic hardening. The stress-strain curves at room temperature of the three different materials which are present in the specimen are provided by project partners. Figure 1 illustrates the plastic behaviour of the different materials at room temperature.

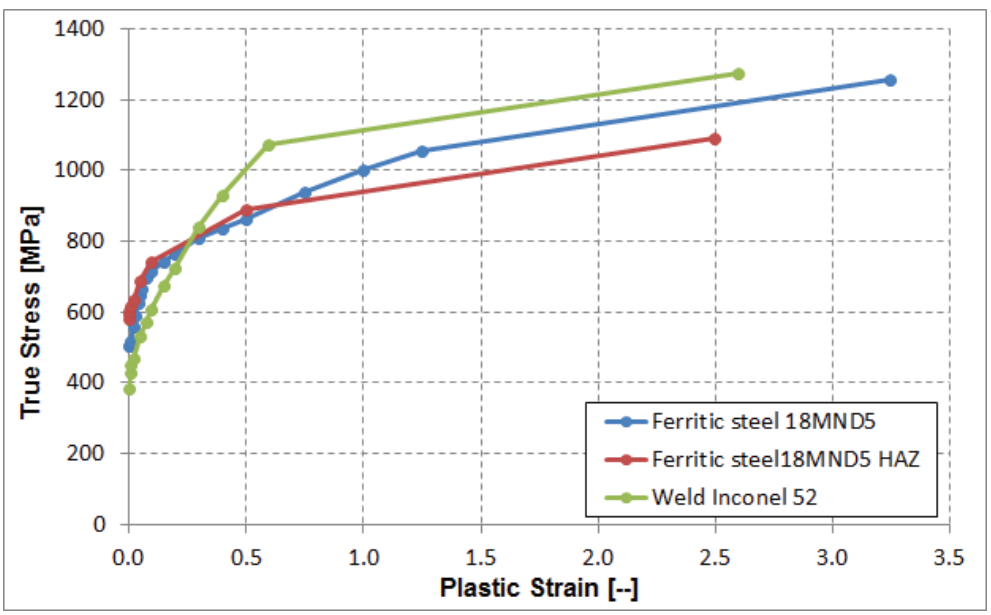

Figure 1. Stress strain curves adopted for the numerical analysis

The loading of the specimen is realistically modelled displacement controlled via two rigid shell parts simulating the bolts of the real experiment. Frictionless contact is defined between the rigid shell parts and the pin holes of the specimen model. Figure 2 shows the generated FE-model representing the CT12.5 specimen 2. The mesh is color-coded to indicate the different material sections of the model. The elements in grey represent the ferritic steel 18MND5. The elements in blue represent the heat affected zone of the ferritic steel 18MND5. The elements in brown represent the Inconel 52 weld material.

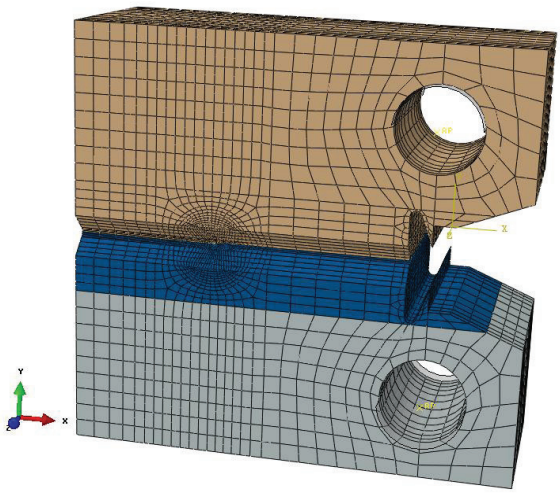

Figure 2. FE-Model of the CT12.5 specimen with mesh and material assignments

The analysis is performed with a predefined, linearly increasing displacement of one of the rigid shell parts in the direction of the global Y-axis. The magnitude of this displacement corresponds to the load line displacement reached at the end of testing of specimen 2 which was δ_{Pi} = 2.2 mm.

Figure 3 provides a comparison of the global specimen behaviour in terms of load displacement curves coming from the experiment and from the numerical analysis. Material damage which causes a softening of the load displacement curve with increasing load in reality is not considered in the analysis. Therefore, similarity of both curves is maintained only up to the beginning of material damage.

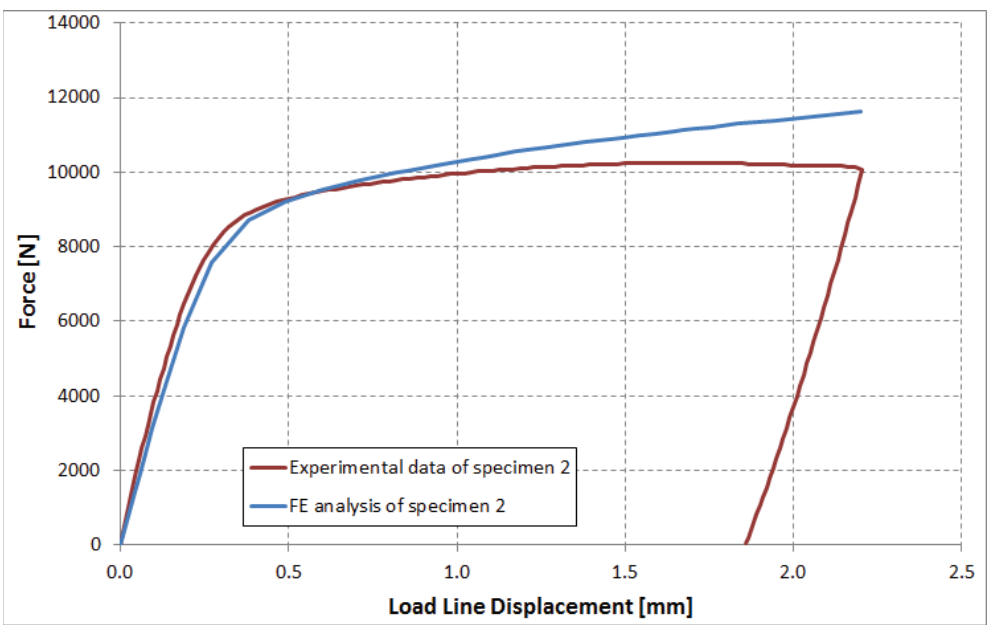

Figure 3. Comparison of experimental and numerical results of global specimen behavior

Figure 4 shows the distribution of equivalent plastic strain at maximum loading. The orientation of the model is equal to Figure 2, ferritic material is located in the lower part of the specimen model. It can easily be seen from this plot that a significant level of plastification is reached in the specimen.

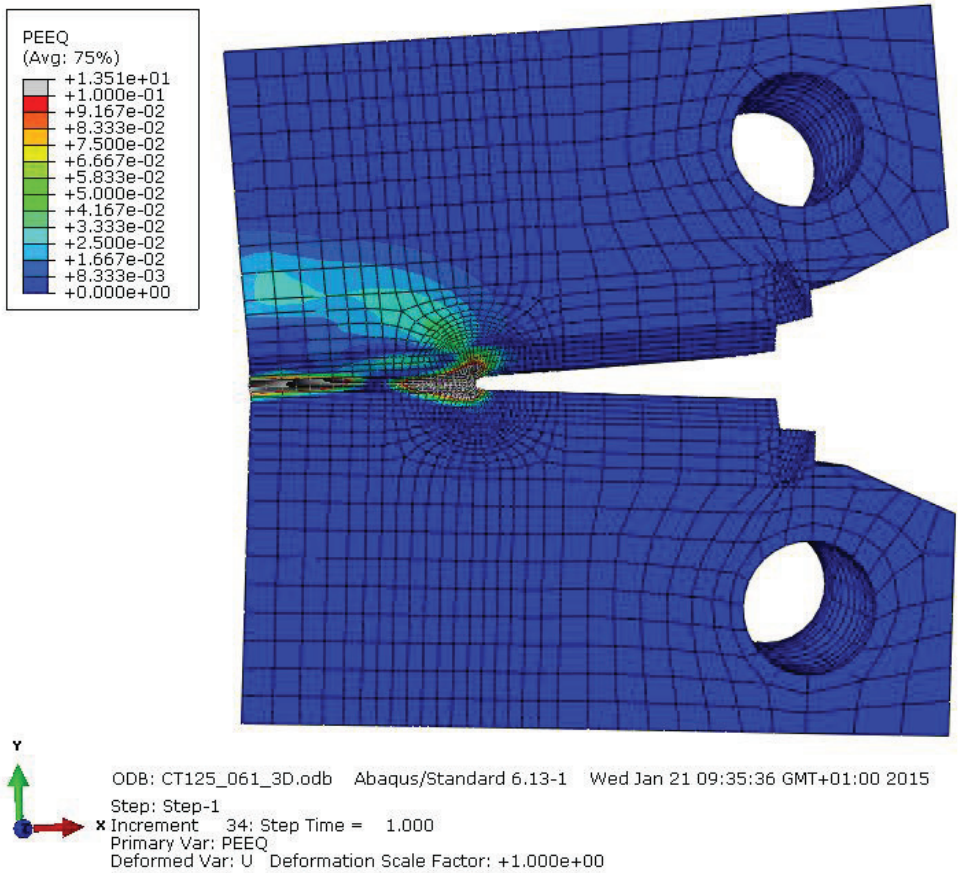

Figure 4. Plot of the FE model showing equivalent plastic strain distribution at maximum loading

Figure 5 depicts the evolution of the J-integral over load line displacement. J-integral is evaluated in the center of the specimen where the crack tip loading is highest over specimen thickness. The experimental value of the J-integral of specimen 2 is given for comparison. It can be seen that the numerical analysis slightly over predicts the experimentally determined value of crack tip loading.

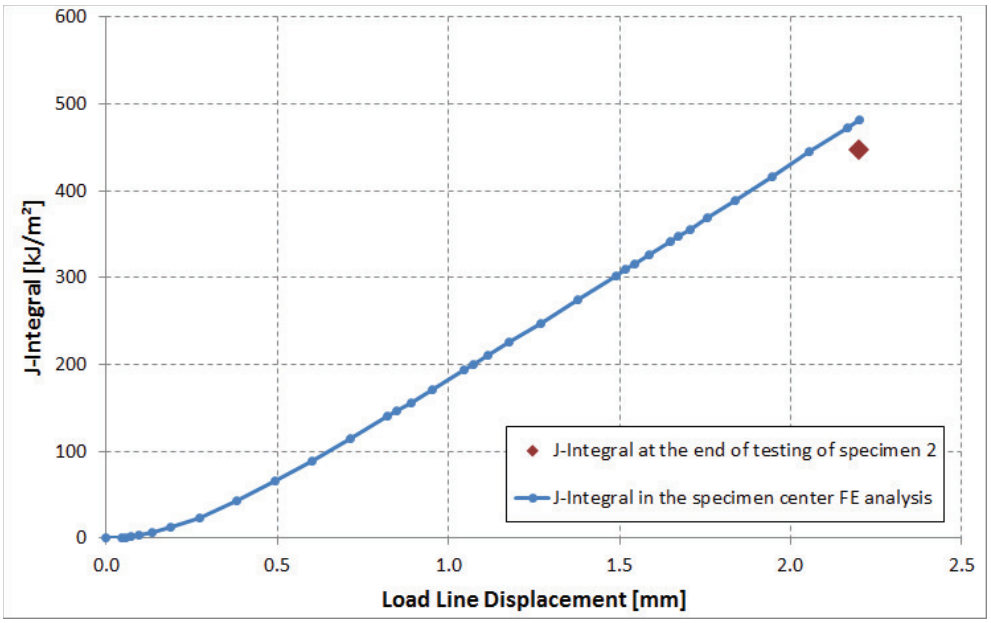

Figure 5. Comparison of numerically calculated J-integral with experimental result

Based on the results of the elastic-plastic analysis, a second analysis with linear-elastic material behaviour is performed to determine the elastic component of the J-integral which is indirectly needed for the calculation of the η_{pl}-factor. The η_{pl}-factor is calculated with a rearranged equation from ASTM 1820-11, see equation 1.

$$\eta_{pl} = \frac{J_{pl} * A_{pl}}{B_N * b_0} \tag{1}$$

A_{pl} represents the energy dissipated by plastic deformation during testing. This property is experimentally determined as the area under the force versus displacement curve. In the numerical analysis, this property can directly be evaluated by Abaqus as history output “ALLPD”.

In order to reproduce the loading conditions of the specimen, the force over time history of the elastic-plastic analysis is used as prescribed loading for the linear-elastic analysis. The elastic J-integral is evaluated via the same path as in the elastic-plastic analysis.

The plastic component of the J-integral which is needed for calculating η_{pl} is determined by subtracting the elastic component from the total value of the J-integral, see equation 2:

$$J_{pl} = J - J_{el} \tag{2}$$

Figure 6 depicts the η_{pl}-factor versus loading in terms of load line displacement. At low loading levels, η_{pl} oscillates due to inaccuracies in the calculation of the plastic component of the J-integral. With increasing J_{pl}, η_{pl} converges to a stable value which is considered the η_{pl}-factor.

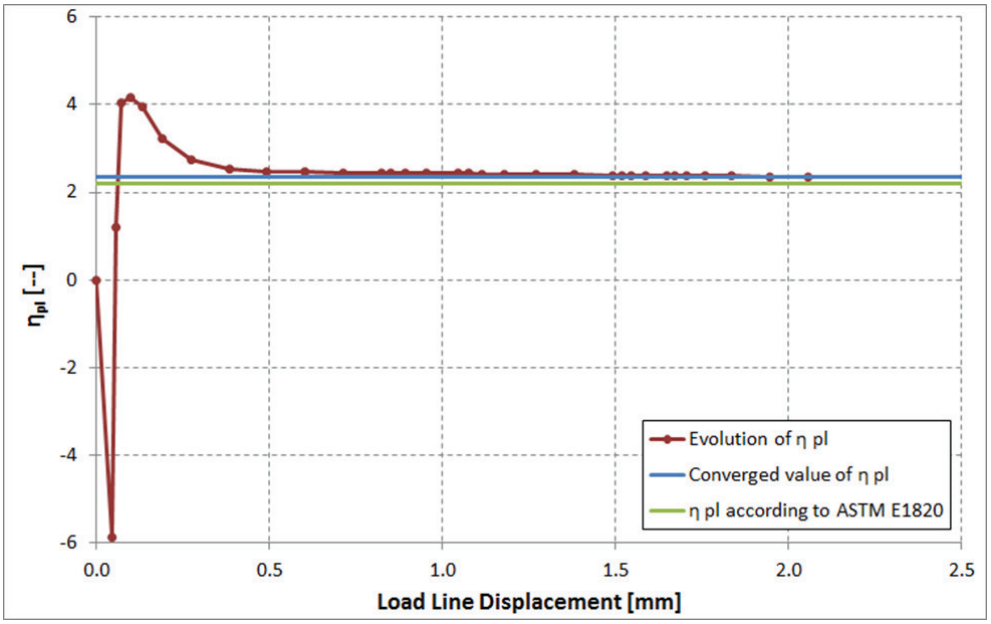

Figure 6. Comparison of numerically calculated η_{pl}-factor and the ASTM E1820 value

Table 1 summarizes the results of the numerical analysis of specimen 2. The experimental results are given as well. It can be seen that the numerical results lead to bigger η_{pl}-factor than the equation for compact specimens given in ASTM 1820-11 which is conservative in terms of the resulting plastic component of the J-integral. This leads to lower J for the material which is penalizing for safety analysing by lowering the apparent toughness. This means also that higher J will be obtained using detailed numerical approach.

Table 1: Comparison of experimental and numerical results

Property	Experiment specimen 2	Numerical analysis
$J(\delta_{Pi})$ [kJ/m²]	448	481
η_{pl} [--]	2.20	2.35

DISCUSSION

Large plastic deformation occurs in the specimen, and plastic strain is not confined to the crack tip but develops into the material with lower yield level for increasing load. Slip lines are seen during experimental testing and ductile tearing and plastic collapse are in competition. Limit load is achieved before tearing initiation. These results indicate that the failure of tough steels when the crack extends in a slow-stable-ductile manner is a plastic tearing problem governed essentially by material properties instead of a "fracture" problem determined by singularity or weak singularity parameters. For specimen 2, we are in a situation of undermatch M < 1 (σ_{ys} weld / σ_{ys} base metal HAZ = 385 / 581 i.e. 0.66). The deformation pattern is that the plastic deformation is mainly occurring in the weld metal, which is obvious since M is small. Many estimations of the limit load are proposed depending upon the selected stress state (plane stress or plane strain conditions) and the plasticity criterion (Tresca or Von Mises criterion). A comparison of several limit load solutions for homogeneous CT-specimen is shown in Figure 7.

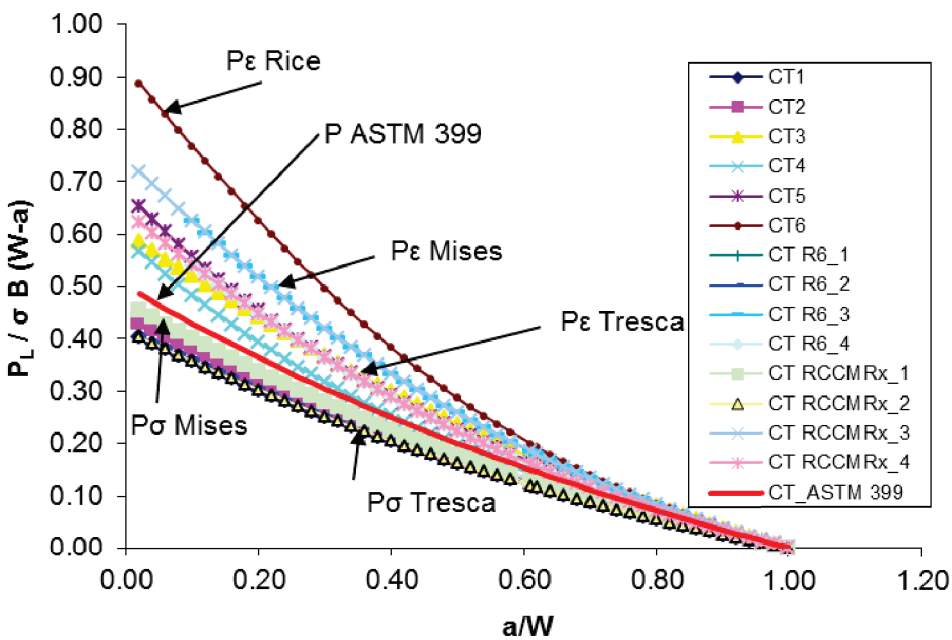

Figure 7. Comparison of limit load solution for homogeneous CT-specimen

The comparison of limit loads assuming the plate is wholly made of base material HAZ $F_{YB\ HAZ}$, or weld F_{YW} are calculated analytically for plane strain with equations from British R6 code (similar to RCC-MRX). The limit load of the DMW F_{DMW} is determined based on the numerical analysis and corresponds to the load at which the slip line field is joining the crack tip to the opposite specimen boundary (limit load scaled on the yield strength). A comparison of the different limit loads is provided in table 2.

Table 2: Plastic limit loads for specimen 2

Source	**Plastic limit load [N]**		
	F_{YW}	**$F_{YB\ HAZ}$**	**F_{DMW}**
R6 code – RCC-MRx (plane strain, Von Mises criterion)	6953	10493	-
Abaqus	-	-	9221

Figure 8 shows three cutaway views of the Inconel 52 part of specimen 2. The plots are taken at different load levels and illustrate the current situation of yielding. All elements in these plots which are not blue coloured are currently under plastic deformation. The plot on the left is taken at the increment when specimen loading reaches the analytically calculated limit load according to table 2. The plots in the middle and on the right are taken at the increments where the plastic zones in the ligament merge. The specimen loading at these increments is considered the plastic limit load F_{DMW} as given in table 2.

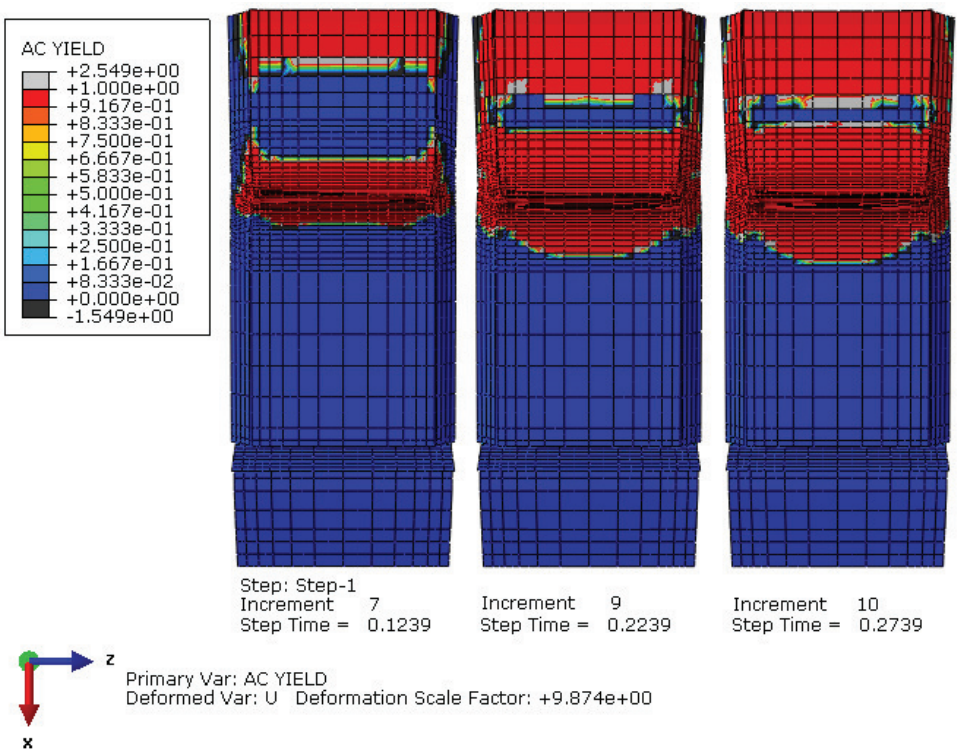

Figure 8. Active plastic zone in the Inconel 52 weld material at three different time increments

The ratio F_{DMW} / F_{DYB} is equal to 0.878 and the ratio F_{DMW} / F_{DYW} = 1.326 considering the lowest FE limit load. Following the investigation performed at GKSS, the limit load can be expressed in term of mismatch for this CT specimen from the MU1 DMW variant with only two materials and with crack located at the interface. This lead to the following solutions for a/W = 0.6:

$$F_{DMW} / F_{YW} = 1.326 \text{ or } F_{DMW} / F_{YW} = 2\ M \quad (3)$$
$$F_{DMW} / F_{YB} = 0.878 \text{ or } F_{DMW} / F_{YB} = 1.33\ M \quad (4)$$

CONCLUSION

The numerical investigation allows us to check the ASTM1820 interpretation of J. In the case of specimen 2, the reults obtained are similar. The numerical investigation allow to obtain the limit load of the non-homogeneous CT specimen, which is similar to the theoretical limit load given by analytical solution scaled on the yield strength of the weakest material. The size requirements of the ASTM 1820 are fulfilled, even using the weakest material (in term of flow stress). However, the experiment show that CT12.5 may be too small to investigate the toughness of MU1 DMW for crack located more than 0.5mm from the fusion line into the Ni-52. Secondary cracks perpendicular to the initial crack plane have been seen. The numerical investigation confirms the ASTM1820 interpretation of J can be used for this DMW CT specimen configuration.

ACKNOWLEDGEMENT

The authors also wish to acknowledge Dr. Mykula Dzubinsky, European Commission DG RTD for his continuous support to the project. This project has received funding from the European Community's Seventh Framework Programme (FP7/2007-2013) under grant agreement n°295968.

NOMENCLATURE

a_0	Initial crack length [mm]
a_m	Machined notch [mm]
ap	Final crack length [mm]
A_P	Plastic area [N*mm]
ASTM	American Society for Testing and Materials
B	Specimen thickness [mm]
b_0	Length of initial ligament [mm]
B_N	Net specimen thickness, sidegrooves [mm]
C_0	Slope at the beginning [mm/N]
C_i	Slope at pop in [mm/N]
C(T)	Compact Tension
E	Young`s modulus [MPa]
$f(a_0/W)$	Form function
F_{DMW}	Limit load for DMW CT specimen
F_{YB}	Limit load assuming CT specimen is wholly made of ferritic base material
F_{YW}	Limit load assuming CT specimen is wholly made of Ni-alloy weld material
J	J-integral [kJ/m²]
J_{el}	Elastic component of J [kJ/m²]
J_{pl}	Plastic component of J [kJ/m²]
K	Critical stress intensity factor [MPa√m]
L	Specimen length [mm]
LLD, δ	Load Line Displacement , displacement [mm]
P	Load [N]
T	Test temperature [°C]
t	Test time [s]
v	Displacement [mm]
W	Specimen width [mm]
Δa	Stable crack growth [mm]
η	Geometric correction factor
ν	Poisson`s ratio
σ_{YS}	Yield Strength [MPa]

REFERENCES

[MULTIMETAL] P Karjalainen-Roikonen, E.Keim, P.Gilles, S.Blasset
"EC FP7 Structural performance of MULTI-METAL component project overview", PVP2013-97574

[ASTM] ASTM Standard ASTM E 1820-11

[Abaqus] Abaqus documentation for version 6.13-1
Dassault Systèmes Simulia Corporation, Providence Rhode Island USA, 2013

[JRC] Martin, Simonovski
Analysis Manual for WP4.2 "K/J Value Estimation of different Specimen Designs"
Part 2a: Multi-Metallic Specimens of Mock-Up 1
Part of Deliverable D4.2, FP7 Project MULTIMETAL, JRC 2014

[Golembiewski] Golembiewski H. J., G.Vazoukis,
Ductility Minimum for Application of Plastic Limit Load Concept to Failure Analysis of Structures with Imperfections, Int. J. Pres. Ves. Piping 24, p. 27 - 36 (1986)

[Chen] Xiaohu Chen "Plastic tearing energy in tough steels"
PhD thesis 2005, University of Maryland

[GKSS] Yun-Jae Kim, Karl-Heinz Schwalbe "Mismatch effect on plastc yield loads in idealized weldment , II. Heat affected zone crack", Engineering Fracture Mechanics 68 (2001) 183-199

References limit load solution for CT-Specimen from figure 7:

CT1 (plane stress)	Merkle, J.G., Corten H.T. A J-integral analysis for the compact specimen, considering axial force as well as bending effects ASME Journal of pressure vessel technology, 1974, pp.1-7
CT2 (plane stress) CT3 (plane strain)	Kumar V., German M.D., Shih C.F. An engineering approach for elastic plastic fracture analysis EPRI, NP-1931 / RP 1237-1, 1981
CT4	W.Schmitt, E.Keim Advances in elasto-plastic fracture mechanics, Applied science publishers Ltd., London, 1980 PP.385-416
CT5	Holstein T., Schmitt W. An estimation procedure for the J-Integral in the fully plastic range - Experimental and analytical verification Int. J. of Fracture 16, 1980, pp. R 195 - R 198
CT6 (plane strain)	Rice J.R. The line spring model for surface flaws, the surface crack: physical problems and computational solutions ed. J.L. Swedlow, ASME New-York 1972
CT R6_1 (plane stress, Von Mises) CT R6_2 (plane stress, Tresca) CT R6_3 (plane strain, Von Mises) CT R6_4 (plane strain, Tresca)	R6 Procedure - Assessment of the integrity of structures containing defects, Rev.4
CT RCC-MRx_1 (plane stress, Von Mises) CT RCC-MRx_2 (plane stress, Tresca) CT RCC-MRx_3 (plane strain, Von Mises) CT RCC-MRx_4 (plane strain, Tresca)	RCC-MRx - Appendix 16